

# RADIOACTIVE NEEDLEWORK

*Reconstruction of needle-positions in radiation treatment*

Claude Archer<sup>1</sup>, Frits van Beekum<sup>2</sup>, Andrew Hill<sup>3</sup>,  
Michiel E. Hochstenbach<sup>4</sup>, and Ionica Smeets<sup>5</sup>

## Abstract

Nucletron presented a medical problem to the SWI 2006: how to find needles used for cancer treatment in a prostate? More concretely: how to find the positions of these needles from distorted images from an ultrasound probe? Section 1 explains the background of this problem. In Section 2 we deal with physical explanations for the distortions. In Section 3 we give a brief overview of medical imaging and explain which techniques we used to clean up the images.

## 5.1 Introduction

Before we state the problem posed by Nucletron, we explain the background of their problem.

### Brachytherapy

In prostate cancer treatment a new therapy has come in use, where, unlike the external radiation in the well-known chemotherapy, the radiation is now supplied by a number of tiny sources *inside* the prostate. Nucletron, with headquarters in Veenendaal, the Netherlands, has developed this *brachytherapy*—brachys is the Greek word for short (here: with respect to distance)—and has been using this medical technology for over five years now.

The short distance between source and target enables a considerable reduction of the dose, thus reducing the risk of damaging the surrounding tissue. Moreover, the distribution of the sources over the prostate is optimised so as to create a prescribed level of radiation over the prostate interior, a higher level

---

1: Haute École Francisco Ferrer, 2: Universiteit Twente, 3: University of Bath, 4: Case Western Reserve University, 5: Universiteit Leiden

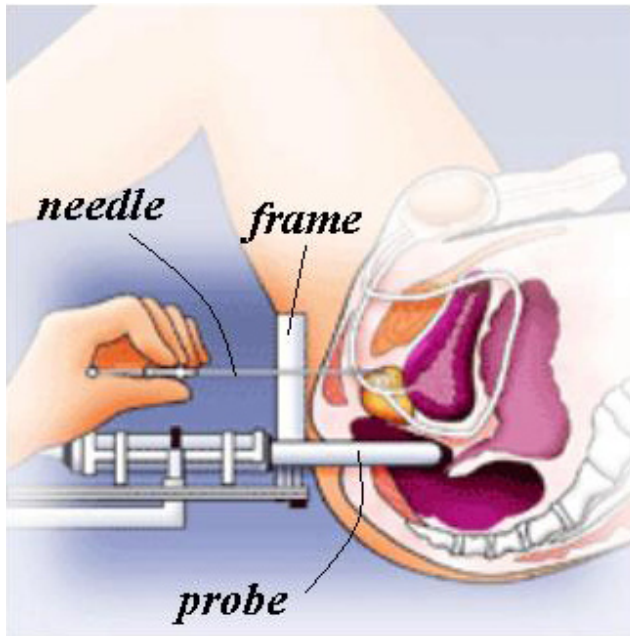


Figure 5.1: Position of the device with frame for inserting the needles and probe for ultrasound monitoring.

near the outer surface, and a lower level near the urethra (which runs right through the prostate).

The sources, so-called seeds, look like pieces of thin pencil-lead and are brought into position through hollow needles with outer diameter 1.25 mm. Typically 2 to 6 seeds are placed in one needle, separated by a dummy or a thread of biodegradable material. The number and spacing of the seeds in each needle and the optimal position for each needle are computed before the operation starts. When the needle has been put in the prostate, this train of seeds is pushed out, while at the same time the needle is withdrawn, thus leaving the seeds and spacers in the desired positions.

The radioactive decay of the used iodine or palladium seeds is such that in half a year the radiation is no more than a few percent. And, although this treatment is not the answer to all types of prostate problems, patients who have been selected for brachytherapy may have good hope that the tumors will disappear and may stay away for 15 years and more.

### **The problems during the operation**

The prostate has the shape and size of a firm walnut, and will be perforated by 12 to 30 needles. The access is through the perineum, which is the skin and tissue between scrotum and anus. A frame containing the needles is positioned

to this perineum. What makes the operation difficult is that the needles, when being pushed in, will not follow the “mathematical” path which is a straight line exactly perpendicular to the frame. In practice, a needle may deviate and make a curve, e.g., because it meets density differences in the tissue or because of play in the frame. Moreover, pushing a needle will affect the position and shape of the prostate itself, so the second needle cannot take the intended position in the tissue even when it would be perfectly perpendicular to the frame.

Due to all this, the calculated optimal distribution of seeds over the needles has become less informative once the needles have been pushed in. Therefore, each time before inserting a needle, the new geometry of the prostate and the position of the needles are measured first. As a result it may be decided to insert one or more extra needles in poorly covered areas. After all this the optimisation procedure is run again and the seed trains are pushed in. To know where the needles are in the body an ultra-sound sensor is used during the treatment.

Running the optimising software takes only one or two minutes, but measuring the new situation is the bottleneck, as it may take approximately fifteen minutes. This is thought to be too long, not only for the doctors and staff who will stand idle in waiting, but also for the patient: the period under anaesthesia should be kept as short as possible. Moreover, due to the perforation the tissue will start swelling, and in fifteen minutes the measured data might have become unreliable. This is another motivation to minimize the measuring time.

## Ultrasound

Measuring the initial situation in the body and monitoring the actions during the operation is done by *ultrasonography* or *ultrasound*. This is a medical imaging technique that uses high frequency sound waves and their echoes. The technique is similar to the echolocation used by bats, whales and dolphins, as well as SONAR used by submarines.

In short, it works as follows\*. From a transmitter at a given point, high-frequency (here: 5 to 7.5 megahertz) sound pulses are sent out into the body. The sound waves travel out and hit a boundary between tissues (e.g., between fluid and soft tissue, soft tissue and needle). Here some of the sound waves get reflected back to the transmitter (which itself can act as a receiver or sensor), while some travel on further until they reach another boundary and get reflected. The reflected waves are picked up by the sensor and relayed to the machine. The machine calculates the distance from the transmitter/sensor to the tissue or organ (boundaries) using the speed of sound in tissue, 1540 m/s, and the time of the echo’s return (usually on the order of millionths of a second). The machine displays the distances and intensities of the echoes on the screen, forming a two dimensional image like the ones shown in Figure 5.1.

---

\*See <http://electronics.howstuffworks.com/ultrasound1.htm>

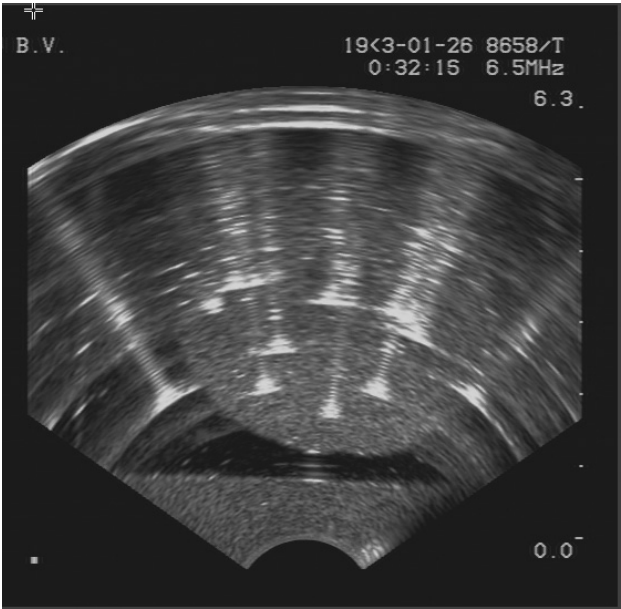


Figure 5.2: A transversal image of the prostate with 12 needles in it. Even the experts at Nucletron had difficulties in identifying them all.

In scanning the prostate, a cylinder-shaped probe of 2 cm diameter is inserted in the rectum. An array of 96 miniature transmitter/sensors covers one quarter of a ring on this cylinder. As each transmitter is assumed to send out signals in a very confined direction perpendicular to the cylinder axis, the probe will scan a 90 degree sector in a plane (slice) transversal to the cylinder. Most of the pictures shown here are transversal scans. A sequence of transversal scans collected by moving the probe up and down in the rectum, can provide 3-dimensional information, from which also other than transversal images can be derived.

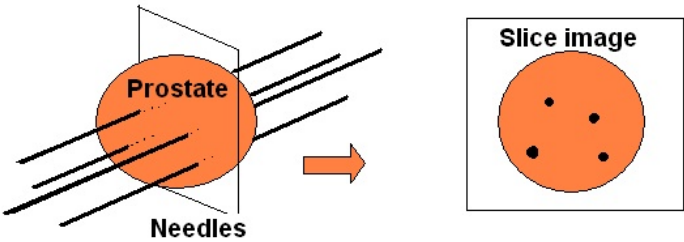


Figure 5.3: Obtaining transversal views of the prostate.

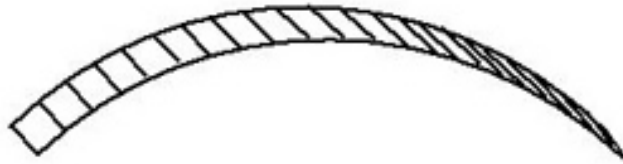


Figure 5.4: An array of 96 transmitters/sensors making one quarter of a “ring” around the cylindrical probe.

### The problem as posed by Nucletron

A typical one-slice scan after inserting a dozen of needles is shown in Figure 5.1. What we want to identify is

- the boundary of the prostate, and
- the location of the needles.

The boundary of the prostate is rather easily seen as a more or less circular interface between two grey levels. Identifying the needles is more difficult. We see several bright spots that no doubt represent a needle, but from further inspecting the figure we can make the following three remarks:

- apart from individual needles we also see some larger bright areas that seem to include two or even three needles (a *cluster*);
- in the “shade” of a needle we see a series of ripples, while there is no physical object there (we will call them *artifacts*);
- if a needle is in the shade of another needle, we cannot see it. This is only natural, but in this case the artifacts seem to make it even more invisible.

With respect to the last remark there is no other remedy than trying to “look around” the nearby needle by changing the position of the probe.

The other two remarks are the core of the questions that Nucletron posed:

- are the artifacts a result of unwanted, but physically real, waves? If so, then what could we physically do about them, rather than suppressing them afterwards by image processing?
- can image processing help to clean up the picture, for instance by suppressing the background noise, decomposing clusters into single needles, suppressing the artifacts, etc., with the ultimate goal to end up with clear needle locations only?

In the next section we go into the details of possible physical explanations for the artifacts. In the last section we deal with medical imaging.

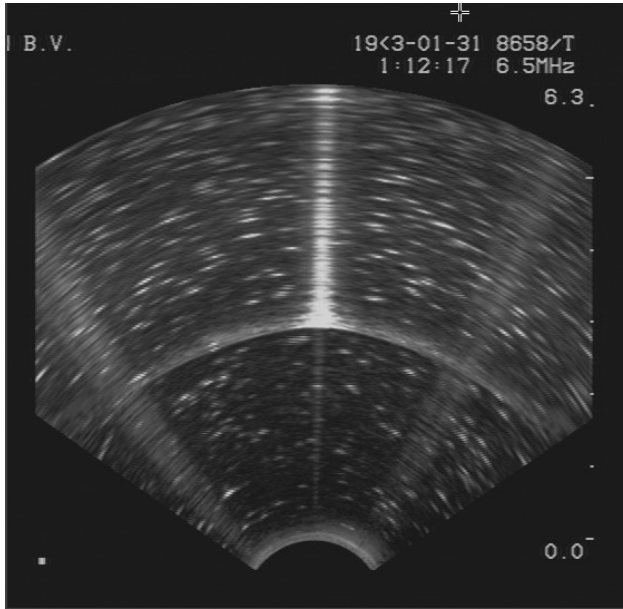


Figure 5.5: Even in a one needle situations artifacts occur.

## 5.2 Physical explanations for the artifacts

For interpretation of the images we have to think of the way the ultrasound works. Each transmitter sends a pulse, and from the time that passes until it receives the echo, it calculates the distance to the reflecting object. A sensor receiving a signal can only draw one conclusion: in the specific direction of this transmitter/sensor there is an object, and its distance is given by the time delay of the signal and the velocity of sound in the medium. Even if the signal would have had multiple reflections on several needles, the interpretation is still a mirroring object on this specific radial line.

However, the multiple needle reflections that we mentioned can not be the cause, as we asked Nucletron to scan a *one needle* situation in the form of a model in a laboratory set-up (i.e., a so-called *phantom* in water). The result is in Figure 5.2, where we still see the same type of artifacts.

Secondly, now restricting to the one needle case, we could think the artifacts might be an interference pattern from two (or more) neighbouring transmitters, reflecting at the same needle. However, the reality of an ultrasound image is that it is a composition of 96 separate images, each showing the echo of *one single transmitter* being active, while all others are silent *and deaf*. So the sensor only receives echoes of its own emitted pulse, no others.

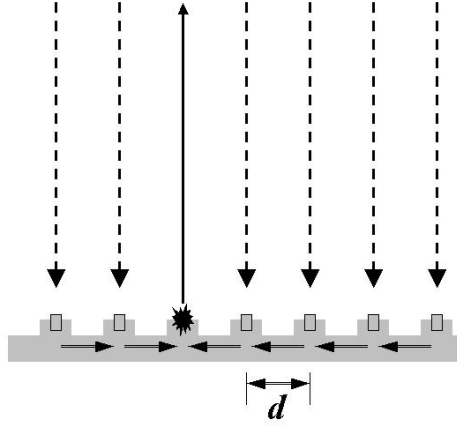


Figure 5.6: Echoes may cause vibrations propagating along the base.

### Two arguments left

Knowing that only one transmitter/sensor is active, and knowing that the spatial pattern of artifacts must be interpreted as signals coming in at subsequent times, the question now is: is there, apart from direct reflection at the needle, any path that a signal can go such that it arrives back at the one and only active sensor at a later time? Can a pulse signal create some vibrations in the region of interest, which will start sending out periodic signals? We guess that here not the soft tissue, but the solid material can come into play: a needle and/or the ring-shaped structure where the sensors are assembled. We start with the latter.

### Vibrations of the probe

If a pulse hits the needle, it will be reflected not only in the direction it originated from, but in a beam of directions. So the reflected signal will not only hit the transmitter it came from, but also the neighbouring ones. Now the neighbouring ones are deaf, so they do not receive the reflected signal. Nonetheless, the reflected signal may make vibrations in the socle (an elevation on which the sensor is mounted). And through the base of the mechanical structure the vibrations will arrive at the active sensor.

A first indication whether this phenomenon can be responsible for the artifacts is in a comparison of the periodicities. The distance  $d$  between two neighbouring sensors is  $1/96$  of one quarter of the perimeter of the probe, which has 2 cm diameter. So  $d = (\pi/4)/96$  times 20 mm, is about 0.16 mm. Now the velocity of sound in the base structure is three times higher than in the tissue. So in the scan image the stripings must have a distance of one third

of 0.16 mm, that is about 0.05 mm. About 600 of these fit in one prostate diameter of (say) 3 cm. However, just by counting in a scan image we find some 50 stripings go in one prostate diameter. So we must conclude that vibrations in the probe do not explain the artifacts.

**Remark.** Maybe the reflected signal could be prevented from hitting neighbouring transmitters if they themselves would send out an exactly counter-phased signal. However, phase control is hardly found in medical applications yet. In cardiology, working with a phased array is in development, but not yet operational.

The ratio 600/50, which is 12, leads us to the idea to search for vibrations on a length scale which is 12 times  $d$ , that is around 2 mm. This length is in the order of the diameter or perimeter of a needle.

### Vibrations of the needle

Is it possible that once hit by the ultrasound wave, the needle starts vibrating and emitting a signal? Such a delayed signal will be interpreted by the probe as an object being behind the needle. This might explain the artifacts.

A way to test this hypothesis is to compute the sound pressure level (SPL) on a needle and then to obtain the resulting displacement  $D$  of the needle. To decide whether such displacement could produce an ultrasound, we have to compare  $D$  to the wavelength of the ultrasound. The 8658 rectal probe used by Nucletron emits and receives 5 to 7.5 MHz signals<sup>†</sup>. Since the velocity of sound in water and human tissues is around 1500 m/s, the corresponding wavelength is around  $1.5 \cdot 10^3 / 5 \cdot 10^6 = 3 \cdot 10^{-4}$  m (300 microns). In section 5.2 we show that the pressure on the needle is completely below that range (by a factor  $10^{15}$ ). Hence the pressure on the needle is  $10^{15}$  times weaker than what is required to produce artifacts. We must conclude that vibrations of the needle do not explain the artifacts.

### Displacement of the needle

The sound pressure level (SPL) in dB is equal to  $20 \cdot \log_{10}(\frac{p_{\text{rms}}}{p_{\text{ref}}})$  where  $p_{\text{ref}} = 10^{-6}$  Pa in water and  $p_{\text{rms}}$  is the *root mean square* pressure. The 8658 rectal probe used by Nucletron has a 60 dB SPL which gives  $p_{\text{rms}} = 10^{60/20} \cdot p_{\text{ref}} = 10^{-3}$  Pa. Let us consider a length  $l$  cylindrical section of the needle (of diameter  $1.5 \cdot 10^{-3}$ ). The density of iron is 7860 kg/m<sup>3</sup>. Hence,

1. only the half part of the needle in front of the wave is submitted to the sound pressure (see [16]). Half of the outer area of the cylinder is  $\pi \cdot l \cdot (1.5/2) \cdot 10^{-3} \text{ m}^2$ . Hence the  $10^{-3}$  Pa pressure produces a force of  $F = \pi \cdot l \cdot (1.5/2) \cdot 10^{-6}$  N on the needle.

---

<sup>†</sup><http://www.bkmed.com/applications/urology/brachytherapy.asp>



2. The mass of the cylinder is  $M = 7860 \cdot \pi \cdot l \cdot (1.5/2)^2 \cdot 10^{-6}$  kg.
3. Let us assume that the position  $X(t)$  of the needle is a harmonic vibration  $X(t) = D \cdot \sin(\omega t)$  where  $\omega = 2\pi f$  and the frequency  $f$  is similar to the frequency of the produced ultrasound (5 to 7.5 MHz). The force on the needle is  $M \cdot X''(t)$  which has magnitude of  $MD\omega^2$ .
4. Combining 1 and 3 we obtain that the displacement of the needle is at most around  $D = F/M\omega^2 = \frac{\pi \cdot l \cdot (1.5/2) \cdot 10^{-6}}{7860 \cdot \pi \cdot l \cdot (1.5/2)^2 \cdot 10^{-6} \cdot 4\pi^2 \cdot 25 \cdot 10^{12}} \approx 2 \cdot 10^{-19}$  m.

Therefore as this vibration displacement must produce an “artifact” ultrasound beam of wavelength around  $3 \cdot 10^{-4}$  m, this fully contradicts the order of magnitude of the effective displacement  $D$  of the needle (a factor  $10^{15}$  difference). As the size of an iron atom is generally estimated around  $3 \cdot 10^{-10}$  m, the displacement of the needle is  $10^9$  times smaller than the iron atom. The emitted ultrasound has not any vibration effect on the needle.

The conclusion of this section must be that until now we do not have a plausible physical explanation for the artifacts. Therefore we move on to mathematical imaging techniques that at least can help to suppress the impact of the artifacts on the screen.

### 5.3 Medical imaging techniques

First we briefly explore the field of medical imaging, after that we explain the techniques we used for cleaning up the images.

#### A short impression and outlook of Mathematical Imaging

Mathematical imaging is a very active research area. Image restoration is the process of attempting to correct for degradation in a recorded image. Several types of problems can be distinguished: image denoising, image deblurring, and image inpainting. We briefly discuss each of these types.

##### Image denoising

In image denoising, the image is degraded by noise, for example during transmission. The model for linear noise is

$$g = f + n,$$

where the vector  $f$  represents the original image,  $n$  is the noise vector, and  $g$  is the vector of the degraded image. The goal of image denoising is the recovery of the original image  $f$  from the degraded image  $g$ . In many applications, a bound  $\|n\|_2 \leq \nu$ , or an estimate  $\|n\|_2 \approx \nu$  for the noise is known, which one may try to exploit.

### Image deblurring

In image deblurring, the continuous model is

$$g(s) = \int_D k(s, t) f(t) dt,$$

where  $D$  is a domain and  $k$  is an integral kernel. In operator form this equation is a Fredholm integral equation of the first kind

$$g = Kf,$$

where the inverse operator  $K^{-1}$  is unbounded. In the discrete case, we would like to find an approximation to the solution  $f$  given discrete, error contaminated data of the form

$$\tilde{g}_j = g_j + n_j,$$

where

$$g_j = g(s_j) = \int_D k(s_j, t) f(t) dt, \quad n_j = n(s_j),$$

and the error  $n$  is discrete white noise, which means that

$$E(n_j) = 0, \quad E(n_i n_j) = \begin{cases} \sigma^2 & i = j, \\ 0 & i \neq j, \end{cases}$$

where  $E$  denotes expectation and  $\sigma^2$  is the variance. Typically, the noise is assumed to be Gaussian distributed, and spatially invariant. Solving for  $f$  given  $g$  is called an inverse problem. These problems are challenging since some regularization technique has to be used to prevent the errors  $n_j$  from blowing up in the solution; therefore this type of problems is called ill-posed (cf., [7]). The most popular choice is Tikhonov regularization, which approximates  $f$  by minimizing an expression of the form

$$\min_f \|Kf - g\|_2^2 + \lambda^2 \|Lf\|_2^2,$$

for a certain regularization parameter  $\lambda$  and regularization operator  $L$ . Often  $L$  is taken to be the identity, while many authors have studied sensible ways to choose  $\lambda$ . One of the alternatives for solving ill-posed systems is formed by the truncated singular value decomposition. Another regularization technique for images is the total variation method [17].

### Image inpainting

In image inpainting part of an image is missing; see [1, 4, 3] for more information.

### Further trends in image processing

We would like to mention a few recent trends in image restoration:

- methods that preserve the edges of the image ([17] and for instance [5]);
- (iterative) methods that preserve the nonnegativity of the pixel values (see [15, 6]);
- restoring images with spatially-variant blur (see [12, 13, 2]);
- the use of point spread functions [12, 18];
- deblurring using multiple images [18];
- the use of subimages [14];
- determining the statistical confidence we can have in the pixel values or features they form in the images [14].

Another relevant field for this project is image registration: determining a geometrical transformation that aligns points in one view of an object with corresponding points in another view of the same object, or a similar object (see [9, 11, 10]). Yet another subfield of imaging is image segmentation, see [8].

### Cleaning up the image

We note that in our case the noise is periodic, and hence in particular spatially variant. In order to identify these periodic patterns Fourier analysis can be used. The Fast Fourier Transform (FFT) decomposes a signal into contribution of waves of particular frequency. The periodic patterns in the image should correspond to a peak in the Fourier transform at the frequency of the pattern. Removing this peak and inverting the Fourier transform will eliminate the patterns which occur at that frequency. The Fourier transform can also be used to remove noise from a signal. In signal processing, noise generally appears as high frequency contributions in the frequency domain. Removing these high frequency contributions produces a cleaned image.

### Coordinate transformation

In order to identify the periodic artifacts we first convert the rectangular coordinate image into polar coordinates. The original image is given in Figure 5.7.

We crop the image to remove the text and focus only on the position of the needles. This results in the image in polar coordinates Figure 5.8

This represents the ultra sound images as measured by the probes. The artifacts now lie in a vertical line behind the needle positions. This change of coordinates allows us to take the Fourier transform in the vertical direction only rather than using a two dimensional transform.

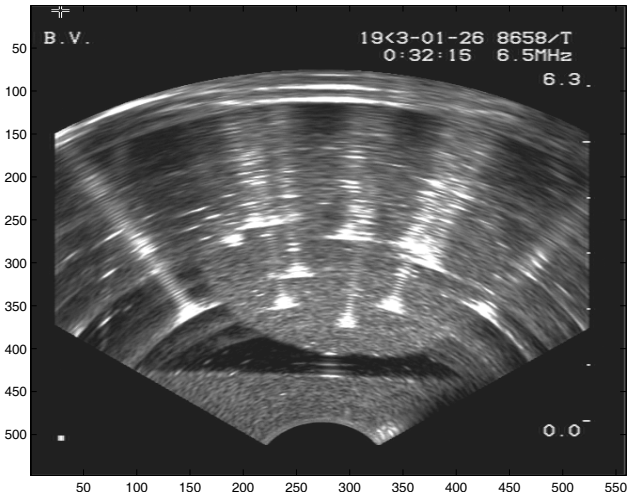


Figure 5.7: The ultra sound image in rectangular coordinates

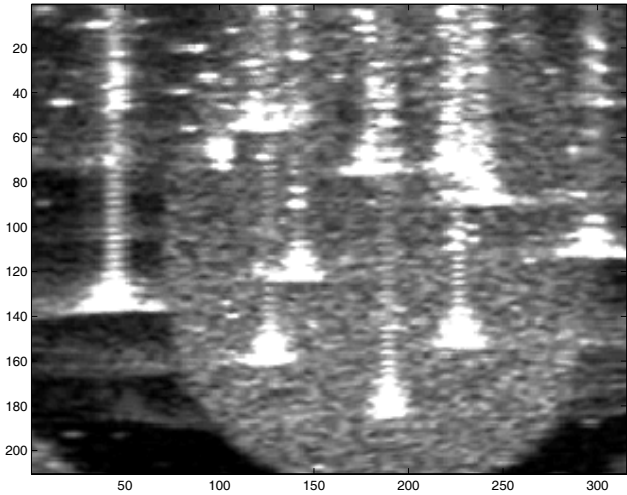


Figure 5.8: The ultra sound image in polar coordinates

**Fourier transform**

Importing the image into Matlab converts the image into a matrix of real valued scalars. The image can now be considered as a series of vertical lines each represented by a vector. The one dimensional discrete FFT is applied to each vector. In the frequency domain we remove all signals above a fixed frequency. This frequency chosen to be large enough to retain the important information in the image, but sufficiently small to remove the periodic artifacts

and denoise the image. The inverse Fourier transform is applied to give the filtered image Figure 5.9.

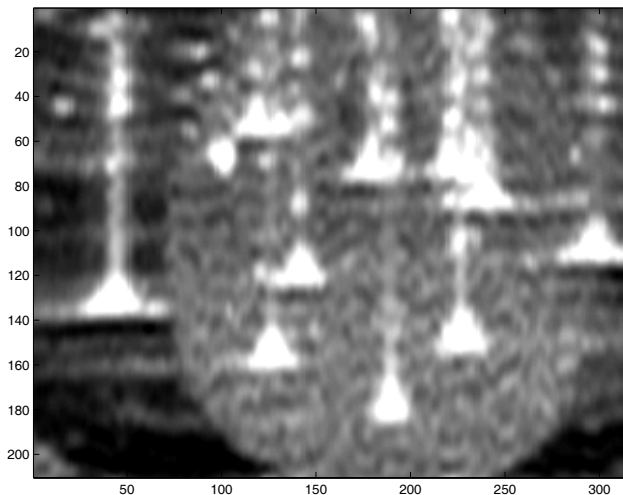


Figure 5.9: The *cleaned* ultra sound image after Fourier analysis

### Thresholding

Finally thresholding can then be applied to the filtered image to aid in identifying the needle positions. Taking a threshold makes a black and white picture from a grayscale picture by making all pixels above a certain value white and all others black. If this value is chosen well, the needles should show up as white blobs in the picture, see Figure 5.10.

**Acknowledgments** We thank Stefan Henn (Heinrich-Heine-Universität Düsseldorf) for his useful comments on the section about medical imaging, Sjoerd Rienstra (Technische Universiteit Eindhoven) for sharing his ideas on the energy argument and Jeroen Schuurmans from Nucletron for bringing us this problem, the time he took to explain all the details to us and his enthusiasm. We also thank Jan Bouwe van den Berg (Vrije Universiteit Amsterdam), Remco Duits (Technische Universiteit Eindhoven), Robbert Fokkink (Technische Universiteit Delft), Erik Franken (Technische Universiteit Eindhoven) and Vivi Rottschäfer (Universiteit Leiden) for their input during the SWI.

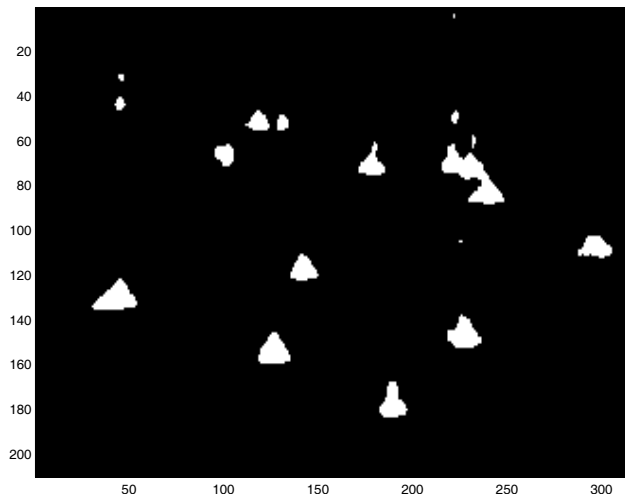


Figure 5.10: The needle positions highlighted using thresholding on the *cleaned* image

## 5.4 Bibliography

- [1] M. BERTALMIO, G. SAPIRO, V. CASELLES, AND C. BALLESTER, *Image inpainting*, in ACM Siggraph, Computer Graphics Proceedings, K. Akeley, ed., 2000, pp. 417–424.
- [2] D. CALVETTI, B. LEWIS, AND L. REICHEL, *Restoration of images with spatially variant blur by the GMRES method*, in Advanced Signal Processing Algorithms, Architectures, and Implementations X; Proc. SPIE Conference, F. T. Luk, ed., vol. 4116, November 2000, pp. 364–374.
- [3] T. F. CHAN, S. H. KANG, AND J. SHEN, *Euler’s elastica and curvature-based inpainting*, SIAM J. Appl. Math., 63 (2002), pp. 564–592.
- [4] T. F. CHAN AND J. SHEN, *Mathematical models for local nontexture inpaintings*, SIAM J. Appl. Math., 62 (2001/02), pp. 1019–1043.
- [5] C. FROHN-SCHAUF, S. HENN, AND K. WITSCH, *Nonlinear multigrid methods for total variation image denoising*, Computing and Visualization in Science, 7 (2004), pp. 199–206.
- [6] M. HANKE, J. G. NAGY, AND C. VOGEL, *Quasi-Newton approach to nonnegative image restorations*, Linear Algebra Appl., 316 (2000), pp. 223–236.
- [7] P. C. HANSEN, *Rank-deficient and discrete ill-posed problems*, SIAM Monographs on Mathematical Modeling and Computation, Society for

- Industrial and Applied Mathematics (SIAM), Philadelphia, PA, 1998. Numerical aspects of linear inversion.
- [8] R. M. HARALICK AND L. G. SHAPIRO, *Image segmentation techniques*, Computer Vision, Graphics, and Image Processing, 29 (1985), pp. 100–132.
  - [9] S. HENN AND K. WITSCH, *Iterative multigrid regularization techniques for image matching*, SIAM J. Sci. Comput., 23(4) (2001), pp. 1077–1093.
  - [10] ———, *Image registration based on multiscale energy information*, SIAM Journal on Multiscale Modeling and Simulation (MMS), 4(2) (2005), pp. 584–609.
  - [11] J. MODERSITZKI, *Numerical methods for image registration*, Numerical Mathematics and Scientific Computation, Oxford University Press, New York, 2004. Oxford Science Publications.
  - [12] J. G. NAGY AND D. P. O’LEARY, *Fast iterative image restoration with a spatially-varying PSF*, in Advanced Signal Processing: Algorithms, Architectures, and Implementations VII; Proc. SPIE Conference, F. T. Luk, ed., vol. 3162, October 1997, pp. 388–399.
  - [13] ———, *Restoring images degraded by spatially variant blur*, SIAM J. Sci. Comput., 19 (1998), pp. 1063–1082.
  - [14] ———, *Image restoration through subimages and confidence images*, Electron. Trans. Numer. Anal., 13 (2002), pp. 22–37.
  - [15] J. G. NAGY AND Z. STRAKOS, *Enforcing nonnegativity in image reconstruction algorithms*, in Mathematical Modeling, Estimation, and Imaging; Proc. SPIE Conference, D. C. Wilson, H. D. Tagare, F. L. Bookstein, F. J. Preteux, and E. R. Dougherty, eds., vol. 4121, October 2000, pp. 182–190.
  - [16] S. W. RIENSTRA AND A. HIRSCHBERG, *Elements of aero-acoustics*, Lecture Notes of Von Karman Lecture Series, (1994).
  - [17] L. I. RUDIN, S. OSHER, AND E. FATEMI, *Nonlinear total variation based noise removal algorithms*, Physica D, 60 (1992), pp. 259–268.
  - [18] R. VIO, J. G. NAGY, AND W. WAMSTEKER, *Multiple-image composition and deblurring with spatially-variant PSFs*, Astronomy & Astrophysics, 434 (2005), pp. 795–800.

